

# Role of Particle Angularity on the Mechanical Behavior of Granular Mixtures

H. Shin<sup>1</sup> and J. C. Santamarina<sup>2</sup>

**Abstract:** Particle shape affects the mechanical behavior of soils, including packing density, stiffness, volume change during shear, and strength. Laboratory experiments conducted to study the mechanical response of sand mixtures made of round and angular grains show an increase in void ratio, small strain shear modulus  $G_{\max}$  (constant fabric), oedometric compressibility  $C_C$  (fabric changes), and friction angle but a decrease in lateral stress coefficient  $k_0$  as the mass fraction of angular particles increases. These results reflect variations in particle mobility and highlight the relative role of contact stiffness versus fabric changes. DOI: 10.1061/(ASCE)GT.1943-5606.0000768. © 2013 American Society of Civil Engineers.

**CE Database subject headings:** Particles; Shape; Coefficients; Earth pressure; Shear waves; Wave velocity; Granular media; Mixtures; Mechanical properties; Compression.

**Author keywords:** Particle shape; Mixture; Coefficient of earth pressure at rest; Shear wave velocity; Compressibility.

## Introduction

Previous studies have explored the origin of particle shape (Cho et al. 2006; Santamarina and Cho 2004), the effect of particle shape on the macroscale mechanical response (eccentricity: Rothenburg and Bathurst 1992; Ting et al. 1993; Aloufi and Santamarina 1995; Guo and Stolle 2006; angularity: Cho et al. 2006; Das et al. 2011; roughness: Santamarina and Cascante 1998; Yimsiri and Soga 1999), and engineering implications (early study by Holubec and D'Appolonia 1972). Results showed that all structural and mechanical properties such as void ratio, stiffness, and friction angle are strongly affected by particle shape characteristics such as sphericity, roundness, and smoothness.

Sediments are granular mixtures made of particles of different size and shape. The behavior of these mixtures is quite complex and may not always be estimated as a linear mass average of the properties of the components. The purpose of this study is to investigate the effect of particle shape on the mechanical properties of sands made of mixtures of angular and round particles.

## Experimental Study

The experimental methodology is described first, followed by a summary of experimental results.

### Materials and Procedures

#### Material and Mixtures

Mixtures of round Ottawa 20–30 sand and angular blasting sand were prepared at selected mass fractions. These sands have the same

mean size ( $D_{50} = 0.7$  mm) and a low coefficient of uniformity ( $C_u = 1.2–1.9$ ) but different particle shapes (Ottawa 20–30: roundness = 0.9 and sphericity = 0.9; blasting sand: roundness = 0.3 and sphericity = 0.55; from Krumbain and Sloss 1963). A total of six mixtures were prepared with different mass fractions of angular blasting sand:  $F_{\text{ang}} = 0, 20, 40, 60, 80,$  and  $100\%$ . All tests were repeated three to five times to assess variability in the dataset.

#### Devices

Horizontal stress and vertical deformation were measured in a soft oedometer cell, and the lateral stress coefficient  $k_0$  and compression index  $C_C$  (cell: aluminum; thickness of 0.13 mm; inner diameter = 66 mm) were computed. Strain gauges were located at mid-height of the sample, as detailed in Shin and Santamarina (2009). The vertical stress range is limited to  $\sigma_v \approx 50$  kPa to keep the circumferential strain  $< 10^{-5}$  so the error in  $k_0$  is less than 0.01 (Okochi and Tatsuoka 1984). The bottom and top plates included bender elements to generate and detect S-waves (vertical propagation, horizontally polarized).

#### Procedure

The homogeneous mix was scooped into a small funnel (tube inner diameter = 4 mm) and slowly rained into the oedometer cell from a height of  $\sim 30$  mm while steadily moving the funnel parallel to the sediment surface. The complementary angle of repose measurements were determined using the same sample preparation method but in a transparent prismatic box (procedure in Santamarina and Cho 2001; detailed discussion in Chik and Vallejo 2005).

## Experimental Results

### Initial Void Ratio

Plotted data correspond to the void ratio measured at the beginning of each oedometric test [Fig. 1(a)]. The rectangular regions show the  $e_{\min} - e_{\max}$  range for Ottawa ( $F_{\text{ang}} = 0\%$ ) and blasting sands ( $F_{\text{ang}} = 100\%$ ); the specimen preparation method used in this study produces sands of medium relative density.

<sup>1</sup>Assistant Professor, School of Civil and Environmental Engineering, Univ. of Ulsan, Ulsan 680-749, South Korea (corresponding author). E-mail: shingeo@ulsan.ac.kr

<sup>2</sup>Professor, School of Civil and Environmental Engineering, Georgia Institute of Technology, Atlanta, GA 30332.

Note. This manuscript was submitted on August 23, 2010; approved on May 13, 2012; published online on May 16, 2012. Discussion period open until July 1, 2013; separate discussions must be submitted for individual papers. This technical note is part of the *Journal of Geotechnical and Geoenvironmental Engineering*, Vol. 139, No. 2, February 1, 2013. ©ASCE, ISSN 1090-0241/2013/2-353-355/\$25.00.

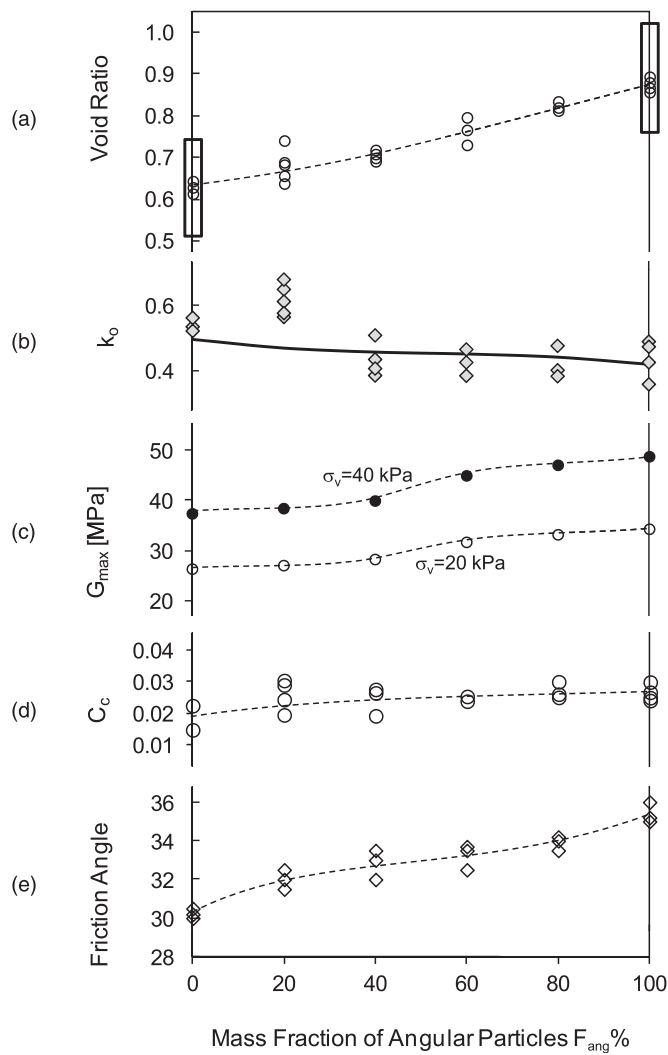


**Fig. 1.** Experimental results: mixture properties as a function of the mass fraction of angular particles  $F_{ang}$ ; (a) void ratio; (b) lateral stress coefficient  $k_0$  (the solid line shows Jaky's equation  $k_0^{<NC>} = 1 - \sin \phi$ ); (c) small strain shear modulus  $G_{max}$  at 20 and 40 kPa; (d) oedometeric compressibility  $C_c$ ; (e) critical state friction angle  $\phi_{cs}$  based on angle of repose

#### Stress Ratio at Rest $k_0$

All specimens exhibited a linear relationship between horizontal  $\sigma_h'$  and vertical  $\sigma_v'$  stresses during the first loading. The stress ratio at rest ( $k_0 = \sigma_h' / \sigma_v'$ ) is plotted for all mixtures in Fig. 1(b).

#### Shear Wave Velocity

The shear wave velocity  $V_S$  was determined at each loading stage during both loading and unloading. Results summarized in Fig. 2 show higher velocity for mixtures with higher fraction of angular particles  $F_{ang}$ . However, they all exhibited a similar velocity-stress gradient. All mixtures were stiffer during unloading.

#### Small-Strain Shear Modulus

The small-strain shear modulus of the soil skeleton ( $G_{max} = \rho V_S^2$ ) was calculated using the measured shear wave velocity  $V_S$  and mass density  $\rho = \rho_m / (1 + e)$ , where  $\rho_m$  is the mass density of the mineral that makes the particles. Data summarized in Fig. 1(c) show the range in  $G_{max}$  values determined at 20 and 40 kPa.

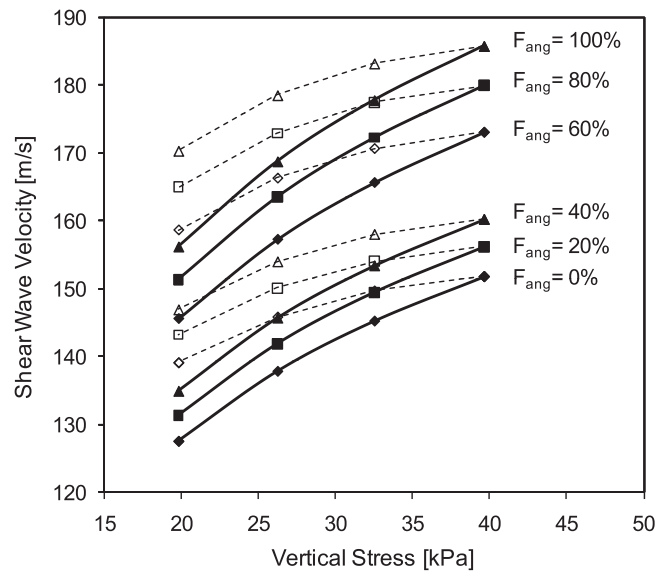


**Fig. 2.** Shear wave velocity versus effective vertical stress during loading (solid lines) and unloading (dashed lines) for different mixtures of angular and round sands

#### Compression Index

The change in void ratio  $\Delta e$  versus the effective stress during the first loading was used to compute the compression index  $C_c = \Delta e / \log(\sigma_{v-max} / \sigma_{v-min})$  [Fig. 1(d)].

#### Friction Angle

The angle of repose was considered a proxy for the critical state friction angle and highlights the role of particle mobility during shear [Fig. 1(e)].

#### Observations

Void ratio  $e$ , shear wave velocity  $V_S$ , small-strain shear modulus  $G_{max}$ , midstrain compressibility  $C_c$  and friction angle  $\phi$  increased with the percentage of angular particles; the opposite was true for the stress ratio at rest during the first loading  $k_0$ .

#### Analyses and Discussion

##### Coefficient of Lateral Stress

The value of  $k_0$  during the first loading was estimated using Jaky's equation (Jaky 1944) and the measured mean angle of repose  $k_0^{<NC>} = 1 - \sin \phi$ . The predicted trend was plotted as a continuous line in Fig. 1(b) and showed good agreement with measured  $k_0$  values, except for the mixture with  $F_{ang} = 20\%$  angular grains. This result may be because of grain mobility and the unique packing configuration often observed in intermediate mixtures (Vallejo 2001).

The value of  $k_0$  increased with increasing overconsolidation ratio (OCR) during unloading.  $k_0^{<OC>} = k_0^{<NC>} OCR^m$  was fit to the experimental data, and  $m \approx 1.1 \sin \phi$  for all mixtures was obtained (typically,  $m = \sin \phi$ ; Mayne and Kulhavy 1982).

##### Velocity-Stress Parameters

A power equation was used to analyze velocity-stress data:

$$V_S = \alpha \left( \frac{\sigma_v + \sigma_h}{2 \text{ kPa}} \right)^\beta = \alpha \left( \frac{1 + k_0}{2} \frac{\sigma_v}{1 \text{ kPa}} \right)^\beta \quad (1)$$

where  $\alpha$  = shear wave velocity at 1 kPa, and  $\beta$  = sensitivity of  $V_S$  to effective stress (i.e., velocity-stress gradient). Empirical parameters  $\alpha$  and  $\beta$  are extracted by fitting Eq. (1) to the loading data using the measured values of  $k_0$ . As observed in Fig. 2, the  $\beta$  exponent is very similar for all mixtures, and the  $\alpha$  factor increases with the percentage of angular particles (Fioravante et al. 1998; Lee et al. 2005).

Trends in Fig. 2 and computed  $\alpha$  and  $\beta$  values appear to contradict standard contact mechanics that anticipates stiffer and less stress-sensitive spherical contacts than conical contacts at constant fabric. These results highlight the role of interparticle coordination and the increase in coordination during loading: contact compliance is compensated by the increase in interparticle coordination between two consecutive load steps (Cascante and Santamarina 1996).

### Stiffness: Small-Strain Shear Modulus $G_{\max}$ versus Oedometric Compressibility

The last observation is in agreement with the higher oedometric compressibility  $C_C$  observed in mixtures with a higher fraction of angular particles  $F_{\text{ang}}$ . The small-strain shear modulus is a constant-fabric measurement of state (instantaneous coordination), whereas oedometric compressibility  $C_C$  is a measure of the skeletal rearrangement and changes in coordination at intermediate strains.

### Comparison with Micaceous Sands

For reference, grain angularity has a much lower effect on packing density, shear stiffness, and oedometric compressibility than the presence of mica platelets in sands (based on data for micaceous sands reported in Gilboay 1928, Gidigas 1976, and Lee et al. 2007).

### Conclusions

Previous studies showed that particle shape factors (i.e., sphericity, roundness, and smoothness) affect the mechanical behavior of soils, including packing density, stiffness, volume change during shear, and strength. Experiments conducted in this study explored the mechanical behavior of mixtures made of round and angular particles.

The presence of angular particles hinders particle mobility, prevents the formation of densely packed sands, leads to a higher friction angle, and lowers the lateral stress coefficient. For comparison, the presence of mica platelets has a more pronounced effect on sands than the effect of angularity.

Mechanical parameters do not vary linearly with the mass fraction of angular particles. In particular, the highest  $k_0$  value (i.e., the closest one to the isotropic stress condition of  $k_0 = 1.0$ ) is measured for mixtures of ~20% angular particles.

The small strain shear modulus  $G_{\max}$  and the compressibility of mixtures  $C_C$  increase with angularity  $F_{\text{ang}}$ . This apparent paradox reminds us that the small-strain shear modulus is a constant-fabric measurement of state (instantaneous particle coordination), whereas oedometric compressibility  $C_C$  is a measure of skeletal rearrangement and changes in coordination at intermediate strains.

### Acknowledgments

Support for this research was provided by the National Science Foundation with additional funding from the University of Ulsan

and the Goizueta Foundation. Connor Barrett and F. Santamarina reviewed and carefully edited the manuscript.

### References

- Aloufi, M., and Santamarina, J. C. (1995). "Low and high-strain macro-behavior of grain masses: The effect of particle eccentricity." *Trans. ASAE*, 38(3), 877–887.
- Cascante, G., and Santamarina, J. C. (1996). "Interparticle contact behavior and wave propagation." *J. Geotech. Eng.*, 122(10), 831–839.
- Chik, Z., and Vallejo, L. E. (2005). "Characterization of the angle of repose of binary granular materials." *Can. Geotech. J.*, 42(2), 683–692.
- Cho, G.-C., Dodds, J., and Santamarina, J. C. (2006). "Particle shape effects on packing density, stiffness, and strength: Natural and crushed sands." *J. Geotech. Geoenviron. Eng.*, 132(5), 591–602.
- Das, N., et al. (2011). "Modeling granular particle shape using discrete element method." *Proc., GeoFrontiers 2011: Advances in Geotechnical Engineering*, ASCE, Reston, VA, 4293–4302.
- Fioravante, V., Jamiolkowski, M., Lo Presti, D. C. F., Manfredini, G., and Pedroni, S. (1998). "Assessment of the coefficient of the earth pressure at rest from shear wave velocity measurements." *Geotechnique*, 48(5), 657–666.
- Gidigas, M. D. (1976). *Laterite soil engineering: Pedogenesis and engineering principles*, Elsevier Scientific, Amsterdam, Netherlands.
- Gilboay, G. (1928). *The compressibility of sand-mica mixtures*, ASCE, Reston, VA, Vol. 54, 2543–2544.
- Guo, P. J., and Stolle, D. F. E. (2006). "Fabric and particle shape influence on  $k_0$  of granular materials." *Soil Found.*, 46(5), 639–652.
- Holubec, I., and D'Appolonia, E. (1972). "Effect of particle shape on the engineering properties of granular soils." *ASTM Spec. Tech. Publ.*, 304–318.
- Krumbein, W. C., and Sloss, L. L. (1963). *Stratigraphy and sedimentation*, 2nd Ed., Freeman and Company, San Francisco.
- Jaky, J. (1944). "The coefficient of earth pressure at rest." *J. Union Hungarian Eng. Architects*, 78(22), 355–358 (in Hungarian).
- Lee, J. S., Fernandez, A., and Santamarina, J. C. (2005). "S-wave velocity tomography: Small-scale laboratory application." *Geotech. Testing J.*, 28(4), 336–344.
- Lee, J. S., Guimaraes, M., and Santamarina, J. C. (2007). "Micaceous sands: Microscale mechanisms and macroscale response." *J. Geotech. Geoenviron. Eng.*, 133(9), 1136–1143.
- Mayne, P. W., and Kulhawy, F. H. (1982). " $k_0$ -OCR relationships in soil." *J. Geotech. Eng. Div.*, 108(6), 851–872.
- Okochi, Y., and Tatsuoka, F. (1984). "Some factors affecting  $k_0$  values of sand measured in triaxial cell." *Soil Found.*, 24(3), 52–68.
- Rothenburg, L., and Bathurst, R. J. (1992). "Micromechanical features of granular assemblies with planar elliptical particles." *Geotechnique*, 42(1), 79–95.
- Santamarina, C., and Cascante, G. (1998). "Effect of surface roughness on wave propagation parameters." *Geotechnique*, 48(1), 129–136.
- Santamarina, J. C., and Cho, G. C. (2001). "Determination of critical state parameters in sandy soils - Simple procedure." *Geotech. Testing J.*, 24(2), 185–192.
- Santamarina, J. C., and Cho, G. C. (2004). "Soil behaviour: The role of particle shape." *Skempton Conf.: Advances in Geotechnical Engineering*, R. J. Jardine, D. M. Potts, and K. G. Higgins, eds., Vol. 1, Thomas Telford, London, 604–617.
- Shin, H., and Santamarina, J. C. (2009). "Mineral dissolution and the evolution of  $k_0$ ." *J. Geotech. Geoenviron. Eng.*, 135(8), 1141–1147.
- Ting, J. M., Khwaja, M., Meachum, L. R., and Rowell, J. D. (1993). "Ellipse-based discrete element model for granular materials." *Int. J. Numer. Anal. Methods Geomech.*, 17(9), 603–623.
- Vallejo, L. E. (2001). "Interpretation of the limits in shear strength in binary granular mixtures." *Can. Geotech. J.*, 38(5), 1097–1104.
- Yimsiri, S., and Soga, K. (1999). "Effect of surface roughness on small-strain modulus: micromechanics view." *Pre-failure Deformation Characteristics of Geomaterials, 2nd Int. Symp.*, M. Jamiolkowski, R. Lancellotta, and D. L. Presti, eds., Balkema, Rotterdam, Netherlands, 597–602.